

Acoustic excitations in glasses close to the breakdown of the continuum approximation

Giulio Monaco*

European Synchrotron Radiation Facility, 6 rue Jules Horowitz, BP 220, 38043 Grenoble Cedex, France

Stefano Mossa†

*UMR 5819 (UJF, CNRS, CEA) CEA, INAC, SPrAM,
17 Rue des Martyrs, 38054 Grenoble Cedex 9, France and*

European Synchrotron Radiation Facility, 6 rue Jules Horowitz, BP 220, 38043 Grenoble Cedex, France

(Dated: January 13, 2019)

The Debye approximation for the acoustic modes in crystalline systems rests on the assumption that the medium is a continuum, holds true for wavelengths much larger than the interatomic spacing and gradually breaks down on approaching the microscopic scale. In glasses, the structural disorder undermines this approximation in a more subtle way. Using molecular dynamics simulations of a model Lennard-Jones glass, we show that the breakdown of the Debye approximation appears in glasses quite abruptly: it shows up as a softening of the acoustic-like excitations on the mesoscopic length-scale of the order of ten interatomic spacings. This feature comes together with a strong scattering regime across which reasonably well defined plane waves transform into a complex pattern of atomic vibrations. This softening turns out to be the direct responsible for the excess found in the specific heat of glasses over the Debye level at low temperatures.

In the macroscopic limit glasses support sound waves as the corresponding crystalline materials do. In fact, averaging on a scale large enough, the details of the microscopic arrangement become essentially irrelevant. This holds true for sound waves with wavelengths up to at least several hundreds of nanometers, as those probed with light scattering techniques [1]. On further decreasing the scale coarsening the effect of the structural disorder must appear. The range of small wavelengths of few nanometers is also well characterized, since it can be accessed experimentally with inelastic x-ray [2] and neutron [3] scattering techniques, and numerically with molecular dynamics simulations [4, 5, 6, 7, 8, 9]. These studies clearly indicate that acoustic-like excitations can still be observed in glasses up to roughly one half of the pseudo Brillouin zone [10] as broad peaks characterized by a dispersion curve that resembles that of the corresponding (poly-)crystals. These acoustic-like excitations are however far from being crystal-like modes and correspond in fact to a complex pattern of atomic motions [5, 6, 7, 8, 9]. Unfortunately, experimental and numerical studies leave a gap between wavelengths of few nanometers and of hundreds of nanometers that is extremely difficult to access. This keeps still open a number of fundamental questions in the physics of glasses: *i)* How does the transition between the large-wavelength Debye-like behaviour and the small-wavelength one look like? In other words, how does it happen that reasonably well defined plane waves transform into a complex pattern of atomic motions that mirror the structural disorder? *ii)* What is the information content that we can extract from the small-wavelength acoustic-like excitations measured in inelastic scattering experiments or calculated numerically? In which properties are their crystal-like features (e.g. existence of pseudo dispersion curves) reflected?

iii) Glasses are known to be characterized by a universal behaviour in some fundamental low-temperature observables like specific heat and thermal conductivity [11]. This is generally related to the ubiquitous existence at energies of a few meV of an excess of modes, known as boson peak, found in the reduced vibrational density of states over the Debye level [12, 13] and whose origin is still lively discussed [14, 15, 16, 17, 18, 19, 20, 21, 22, 23, 24, 25]. Is this universal behaviour related to the nature of the acoustic excitations in the low-frequency range? Or, alternatively, do we have to imagine that glasses are characterized by additional soft, low-frequency modes?

The experiments that have attempted to access this difficult range have lead to contrasting interpretations. An experiment based on a tunnel junction technique reported [26] linear dispersion for the transverse acoustic excitations in silica up to frequencies 50% smaller than the boson peak position in that glass, and excluded any acoustic contribution to the low-temperature anomalies in the specific heat of glasses. Early inelastic x-ray scattering results [2], supported by numerical simulation data [5, 6, 7, 8, 9], seemed to confirm that scenario and showed crystal-like dispersing high-frequency longitudinal acoustic-like excitations with a broadening increasing quadratically with the frequency, thus suggesting a smooth transition between the macroscopic and microscopic regime. More recent inelastic x-ray scattering studies have however revealed that the boson peak marks the energy where a qualitative change takes place: the longitudinal acoustic-like excitations show, below the boson peak position, a softening of the phase velocity [27] and a broadening characterized by a remarkable fourth-power-law frequency dependence [27, 28]. A similarly strong scattering regime for the transverse acoustic modes had been measured in silica at low temperature

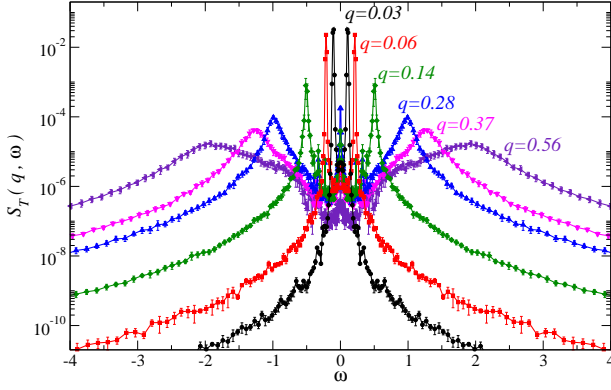


FIG. 1: Transverse dynamical structure factors, $S_T(q, \omega)$, for a LJ glass at number density $\hat{\rho}=1.015$, temperature $T=10^{-3}$ and at the indicated q values, including the smallest one accessible using a simulation box containing $\approx 10^7$ atoms.

and at frequencies below the boson peak position using a tunnel junction technique [29]. Conversely, a recent experiment using inelastic ultraviolet light scattering to measure the longitudinal acoustic modes in silica at room temperature reported the onset of this strong scattering regime at energies one order of magnitude smaller than the boson peak position [30]: the boson peak would then be not directly related to this strong scattering regime.

Classical molecular dynamics studies have not been resolute in this situation up to now due to the fact that the largest wavelengths that can be studied—fixed by the simulation box size and then ultimately by computer power—correspond to few nanometers: the corresponding shortest frequency acoustic-like excitations that are accessible lie then close to the boson peak position, and have not allowed yet for definite conclusions in this supposingly crucial frequency range. Exploiting an exceptionally large simulation box size, we present here results for a model Lennard-Jones (LJ) glass that bridge this gap, and clarify how the acoustic modes look like in the frequency region where the boson peak appears.

The present numerical investigation has been performed using simulation boxes of different sizes containing up to $N \simeq 10^7$ atoms, interacting via a Lennard-Jones potential with periodic boundary conditions. Reduced LJ units are here used. A standard microcanonical classical molecular dynamics simulation, carried out at the constant number density $\hat{\rho}=1.015$ and at temperature $T=2$ in the normal liquid phase is followed by a fast quench ($dT/dt \approx 8 \times 10^2$) down to $T=10^{-3}$. The quenched glass sample is relaxed for a time (dependent on the sample size) sufficient to have a constant total energy. The atomic positions, $\mathbf{r}_i(t)$, and velocities, $\mathbf{v}_i(t)$, have then been stored for a time (again dependent on the sample size) sufficient to get the desired resolution function. The time correlation functions required to obtain the dynamic structure factor, $S_L(q, \omega)$, and its analogous function for

the transverse excitations, $S_T(q, \omega)$ have been computed as:

$$S_\alpha(q, \omega) = \frac{1}{2\pi N} \left(\frac{q}{\omega} \right)^2 \int dt \langle \mathbf{j}_\alpha(q, t) \cdot \mathbf{j}_\alpha^\dagger(q, 0) \rangle e^{i\omega t}. \quad (1)$$

Here α is L or T , $\mathbf{j}_L(q, t) = \sum_{i=1}^N [\mathbf{v}_i(t) \cdot \hat{\mathbf{q}}] \hat{\mathbf{q}} \exp\{i\mathbf{q} \cdot \mathbf{r}_i(t)\}$, $\mathbf{j}_T(q, t) = \sum_{i=1}^N \{\mathbf{v}_i(t) - [\mathbf{v}_i(t) \cdot \hat{\mathbf{q}}] \hat{\mathbf{q}}\} \exp\{i\mathbf{q} \cdot \mathbf{r}_i(t)\}$, and $\hat{\mathbf{q}} = \mathbf{q}/|\mathbf{q}|$. Moreover, a standard normal modes analysis has been carried out to derive the vibrational density of states, $g(\omega)$, from the eigenvalues of the dynamical matrix calculated in the inherent structures of the glass.

In Fig. 1 some representative transverse dynamical structure factor spectra, $S_T(q, \omega)$, are reported, including those corresponding to the lowest q value that we could reach in our simulation. For reference, we recall that at the studied number density the first sharp diffraction peak of the studied glass is at $q_m=7$: the spectra reported in Fig. 1 correspond then to q -values down to $\sim 10^2$ times smaller than the border of the pseudo-Brillouin zone.

The position of the Brillouin peak, Ω_T , in $S_T(q, \omega)$ is utilized to obtain the transverse sound phase velocity, $c_T = \Omega_T/q$, reported in Fig. 2a as a function of the excitation frequency. These data show the already reported positive dispersion of the sound velocity for $\omega > 0.8$ [7]. It is interesting to observe that below that frequency the macroscopic sound velocity limit is not directly recovered but instead a region of softening for the acoustic velocity appears: this is exactly the region where the boson peak is found in this LJ glass [23] (see also Fig. 4 below). The boson peak anomaly then appears in a frequency range where the acoustic-like excitations do not disperse linearly, at odds with what was previously thought [2, 26], but where they experience a more complex dispersion behaviour. In the same panel we also report the results obtained from a normal modes analysis of the glass in its inherent structure [31]. This latter procedure leads to the sound velocity corresponding to the pure transverse acoustic modes (eigenstates of the system), as opposed to that associated to the acoustic-like modes appearing in $S_T(q, \omega)$: it is exact in the $q \rightarrow 0$ limit and can be expected to lead to reasonable results up to $q \sim 0.2-0.3$. For this quantity, the softening discussed above appears even more pronounced, and has been interpreted in terms of the failure of the classical Born approximation for the description of the continuum elasticity in disordered systems [23]. It is clear that the two different routes followed to compute the transverse sound velocity do not lead to the same results in the explored q -range, though at small frequency both of them tend, as expected, to the same, macroscopic value.

The information required to clarify this issue can be found in Fig. 2b, where the frequency-dependence of the broadening (FWHM), $2\Gamma_T$, of the transverse acoustic-like excitations is presented. These data clearly show two different regimes: a ω^2 regime at high-frequencies,

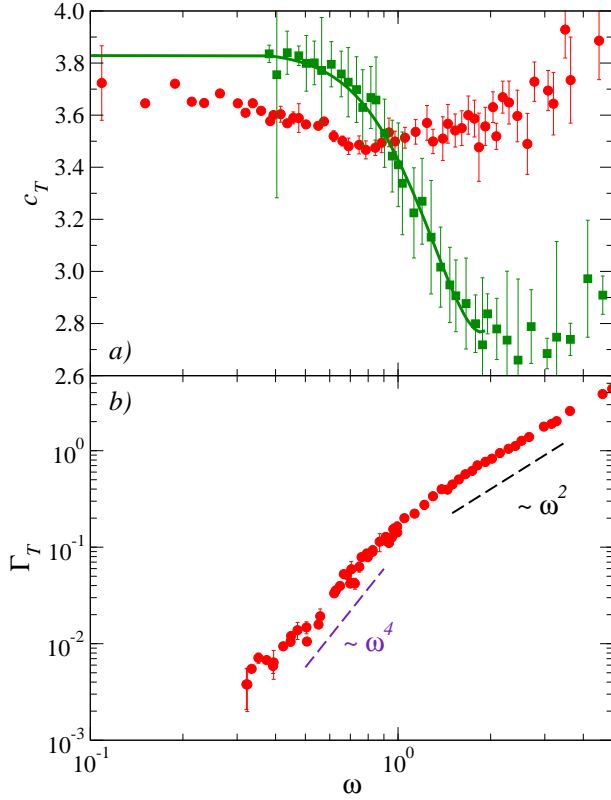


FIG. 2: Phase velocity and broadening of the transverse acoustic-like excitations in a Lennard-Jones glass. Frequency dependence of phase velocity (red circles, panel a) and FWHM (red circles, panel b) of the transverse acoustic-like excitations of the studied LJ glass. These data have been derived by fitting a damped harmonic oscillator model [2] to the transverse dynamic structure factor spectra obtained by molecular dynamics. The dashed lines in b) emphasize different regimes: $\approx \omega^2$ at high-frequencies and $\approx \omega^4$ at low-frequencies. The transition between the two regimes appears at the frequency where the phase velocity in a) shows a minimum. Phase velocity data obtained from the analysis of the normal modes of the glass in the corresponding inherent structure are also reported in a) (green squares) together with the function used to empirically describe their frequency dependence (full line).

as already known from previous studies and associated to the structural disorder of the glass [6, 7, 8], and a ω^4 regime at low frequencies. The frequency that marks the change of regime is very close to, though slightly lower than, the boson peak position (see Fig. 4). Moreover, the low frequency regime appears in the same frequency range where the softening of the sound velocity shows up in Fig. 2a, thus indicating that these two features must be related. This, however, is not surprising if one recalls that a complex self-energy term must be included in the phonon propagator required to describe the reported phenomenology, thus giving rise both to broadening and dispersion of the acoustic-like excitations. This observation in turn can help to explain the results reported in Fig. 2a: the normal modes analysis allows us to identify

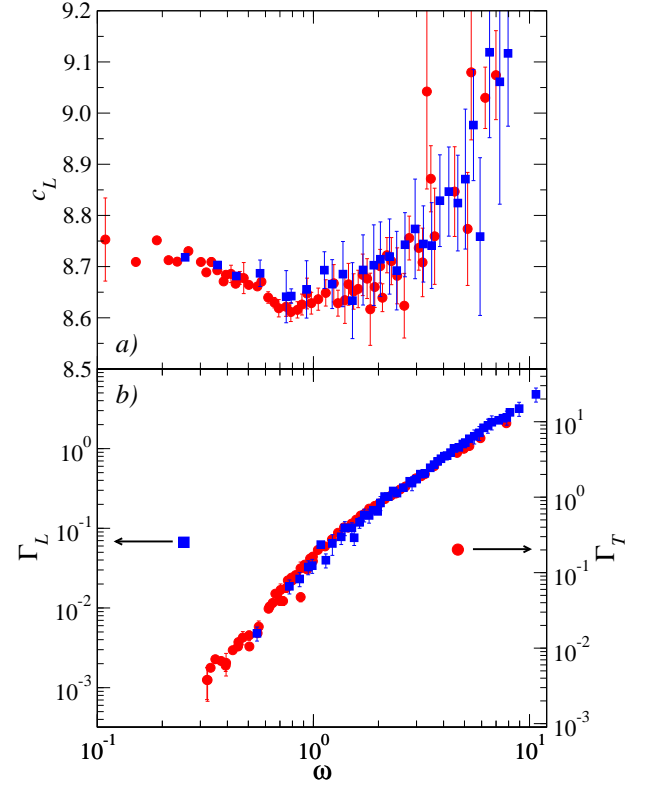


FIG. 3: Comparison between transverse and longitudinal acoustic-like excitations in a Lennard-Jones glass. Frequency dependence of phase velocity (blue squares, panel a) and broadening (blue squares, panel b, left axis) of the longitudinal acoustic-like excitations of the studied LJ glass. These data, similarly to those in Fig. 2, have been derived by fitting a damped harmonic oscillator model to the longitudinal dynamic structure factor spectra obtained from molecular dynamics. In panel a) the longitudinal phase velocity data are compared to those calculated from the corresponding transverse ones (red circles) assuming a frequency-independent bulk modulus $B=59$. Within error-bars, we can conclude that the frequency-dependence of the longitudinal phase velocity directly reflects that of the transverse one. In panel b) the longitudinal excitations broadening data are compared to the corresponding transverse ones (red circles, right axis): the two sets of data can be convincingly scaled one on top of the other. Within error-bars, we can again conclude that the frequency-dependence of the longitudinal data directly reflects that of the transverse ones.

the sound velocity of the purely acoustic modes (eigenstates of the system) while the molecular dynamics data can be considered as average values over the distribution of modes reflected by the broadening of the acoustic-like excitations in $S_T(q, \omega)$.

A similar scenario holds as well for the longitudinal acoustic-like modes. The longitudinal sound velocity data (blue squares) are reported in Fig. 3a where they are compared to the estimation (red circles) based on the

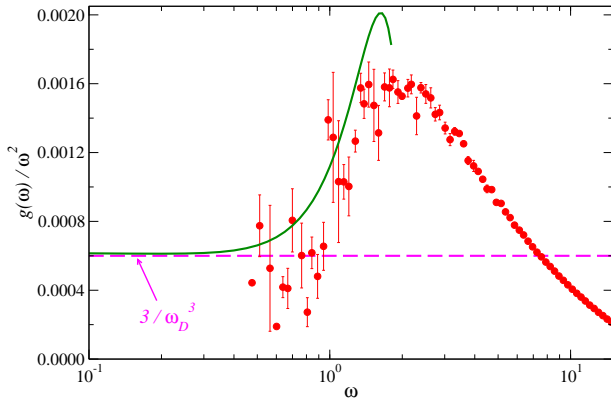


FIG. 4: Reduced density of states obtained from the analysis of the normal modes of the studied LJ glass in its inherent structures (red circles) showing the boson peak at $\omega \simeq 2$. The macroscopic, Debye limit (dashed horizontal line) is indicated as well. The reduced density of states directly obtained from the dispersion curve of the transverse modes via Eq. 3 is reported (full green line) up to the maximum frequency where this analysis is appropriate. The agreement between the two calculations is good – note that there is no adjustable parameter in this comparison. This implies that the density of states, up to and including the boson peak, is of purely acoustic origin.

transverse data reported in Fig. 2a using the relation:

$$c_L(\omega) = \sqrt{\frac{B}{\rho} + \frac{4}{3}c_T^2(\omega)}, \quad (2)$$

where ρ is the mass density. A value $B=59$ for the frequency independent bulk modulus has been obtained from the low-frequency data for $c_L(\omega)$ and $c_T(\omega)$ and it is in good agreement with the literature value obtained for a slightly different system [23]. The good correspondence between the two sets of data in Fig. 3a thus strongly supports a scenario where the bulk modulus is frequency independent and where the frequency dependence of the longitudinal sound velocity simply derives from that of the transverse one. This picture is further reinforced by the comparison shown in Fig. 3b between the broadening (FWHM) of the longitudinal acoustic-like excitations (blue squares, left axis) and that of the transverse ones (red circles, right axis). It is clear here that these two quantities, within error-bars, can be scaled one on top of the other. This confirms that, within the accuracy of our calculations, the frequency dependence that characterizes the longitudinal acoustic-like excitations comes into play through the shear component of the longitudinal response, while the bulk component is a mere spectator.

The present results show clearly that the macroscopic and microscopic regimes are connected by a crossover region where the acoustic branches show a considerable softening—this directly testifies the existence of an abrupt breakdown of the Debye approximation in glasses [27].

This comes together with the signature of strong scattering for the acoustic-like excitations across which reasonably well defined plane waves transform into a complex pattern of atomic vibrations. The connection to the boson peak is clear as well: a softening of the transverse and longitudinal sound velocities directly implies an excess in the reduced vibrational density of states above the Debye level. Since this softening directly appears in the range where the boson peak is observed, or at the corresponding temperatures where the excess in the specific heat universally appears in glasses [11], we can then conclude that these anomalies must have an acoustic contribution. The preceding results confirm as well that the Ioffe-Regel limit for the transverse excitations, defined as the frequency where $\Omega_T = \pi\Gamma_T$, is located in glasses at the boson peak position [25]. It is also clear that the Ioffe-Regel limit is reached at different frequencies for the longitudinal and transverse excitations, and that the longitudinal one shows up at frequencies slightly higher than the boson peak position [25]. However, it is important to underline that this last result seems not to be general: in a simulation study of a silica glass the Ioffe-Regel crossover was found to appear at the same frequency for both polarizations [6].

We now discuss the implications of the preceding results for the vibrational density of states that we calculate from a normal modes analysis and report in Fig. 4 (red circles). In fact, it is easy to directly estimate the acoustic contribution to the vibrational density of states starting from the knowledge of the dispersion curves. In a simple plane-wave approach:

$$\begin{aligned} \frac{g(\omega)}{\omega^2} &= \frac{1}{q_D^3} \left[\left(\frac{q^2}{\omega^2} \frac{\partial q}{\partial \omega} \right)_L + 2 \left(\frac{q^2}{\omega^2} \frac{\partial q}{\partial \omega} \right)_T \right] \\ &\simeq \frac{3}{q_D^3} \left(\frac{c_T}{c_D} \right)^3 \left(\frac{q^2}{\omega^2} \frac{\partial q}{\partial \omega} \right)_T, \end{aligned} \quad (3)$$

where L and T stand for the longitudinal and transverse polarization; q_D and c_D are the Debye wavenumber and velocity, respectively. The approximation on the right hand side of Eq. 3 is justified by the fact that the longitudinal contribution to the total vibrational density of states is small since it scales with $c_T^3/(2c_L^3)=4\%$. It is clear that in order to follow this approach we shall use the dispersion curve obtained from the normal mode analysis, since in that case the low-frequency acoustic modes are reasonably close to being plane waves. In order to compute Eq. 3, instead of directly differentiating the transverse dispersion curve, we prefer to use an empirical model to fit the simulation data (full line through the points in Fig. 2a) and then to differentiate the model function. The result of this calculation is shown in Fig. 4 (full line) and, as it can be appreciated, it well describes the boson peak. It is worth underlining that no additional input but the knowledge of the dispersion curve is required to perform this calculation. It is then clear

that the reduced density of states of the studied glass, up to and including the boson peak, is of purely acoustic origin.

Summing up, the present simulation results shed new light on the well known universal anomaly observed in the specific heat of glasses in the $T \sim 10$ K temperature range and related to the boson peak in the vibrational density of states. While almost all of the existing analyses of these properties assumed that the Debye approximation is valid and discussed the anomalies in terms of the scattering of sound waves, we show here that the breakdown of the Debye approximation on the mesoscopic scale is at the origin of these anomalies, that can be finally traced back onto the elastic properties specific of glasses.

We thank A. Tanguy for discussions.

* gmonaco@esrf.fr

† stefano.mossa@cea.fr

- [1] S. M. Shapiro, R. W. Gammon, and H. Z. Cummins, Appl. Phys. Lett. **9**, 157 (1966).
- [2] F. Sette, M. Krisch, C. Masciovecchio, G. Ruocco, and G. Monaco, Science **280**, 1550 (1998).
- [3] L. E. Bove *et al.*, Europhys. Lett. **71**, 563 (2005).
- [4] G. S. Grest, S. R. Nagel, and A. Rahman, Phys. Rev. Lett. **49**, 1271 (1982).
- [5] V. Mazzacurati, G. Ruocco, and M. Sampoli, Europhys. Lett. **34**, 681 (1996).
- [6] S. N. Taraskin and S. R. Elliott, J. Phys. Condens. Matter **11**, A219 (1999).
- [7] G. Ruocco *et al.*, Phys. Rev. Lett. **84**, 5788 (2000).
- [8] J. Horbach, W. Kob, and K. Binder, Eur. Phys. J. B **19**, 531 (2001).
- [9] H. R. Schober, J. Phys. Condens. Matter **16**, S2659 (2004).
- [10] G. S. Grest, S. R. Nagel, and A. Rahman, Phys. Rev. B **R29**, 5968 (1982).
- [11] W. A. Phillips ed., *Amorphous solids: low temperature properties* (Springer, Berlin)(1981).
- [12] U. Buchenau, N. Nücker, and A. J. Dianoux, Phys. Rev. Lett. **53**, 2316 (1984).
- [13] V. K. Malinovsky, V. N. Novikov, and A. P. Sokolov, Phys. Lett. A **153**, 63 (1991).
- [14] V. G. Karpov, M. I. Klinger, and F. N. Ignat'ev, Sov. Phys. JETP **57**, 439 (1983).
- [15] M. Dove *et al.*, Phys. Rev. Lett. **78**, 1070 (1997).
- [16] W. Schirmacher, G. Diezemann, and C. Ganter, Phys. Rev. Lett. **81**, 136 (1998).
- [17] B. Hehlen *et al.*, Phys. Rev. Lett. **84**, 5355 (2000).
- [18] S. N. Taraskin, Y. L. Loh, G. Natarajan, and S. R. Elliott, Phys. Rev. Lett. **86**, 1255 (2001).
- [19] J. P. Wittmer, A. Tanguy, J.-L. Barrat, and L. Lewis, Europhys. Lett. **57**, 423 (2002).
- [20] V. L. Gurevich, D. A. Parshin, and H. R. Schober, Phys. Rev. B **67**, 094203 (2003).
- [21] V. Lubchenko and P. G. Wolynes, Proc. Natl. Acad. Sci. USA **100**, 1515 (2003).
- [22] T. S. Grigera, V. Martín-Mayor, G. Parisi, and P. Verrocchio, Nature **422**, 289 (2003).
- [23] F. Leonforte, R. Boissière, A. Tanguy, J. P. Wittmer, and J.-L. Barrat, Phys. Rev. B **72**, 224206 (2005).
- [24] W. Schirmacher, Europhys. Lett. **73**, 892 (2006).
- [25] H. Shintani and H. Tanaka, Nature Mater. **7**, 870 (2008).
- [26] M. Rothenfusser, W. Dietsche, and H. Kinder, Phys. Rev. B **27**, 5196 (1983).
- [27] G. Monaco and V. Giordano, Proc. Natl. Acad. Sci. USA, in the press (2009).
- [28] B. Rufflé, G. Guimbrètière, E. Courtens, R. Vacher, and G. Monaco, Phys. Rev. Lett. **96**, 045502 (2006).
- [29] W. Dietsche and H. Kinder, Phys. Rev. Lett. **43**, 1413 (1979).
- [30] C. Masciovecchio *et al.*, Phys. Rev. Lett. **97**, 035501 (2006).
- [31] The dispersion curve corresponding to the transverse eigenstates of the system has been constructed as in Ref. [23], i.e. collecting the lowest four degenerate eigenvalues (all of transverse polarization) obtained from the diagonalization of the dynamical matrix corresponding to simulation boxes of different sizes and using a geometrical criterion based on their degeneracy to associate the obtained eigenvalues to specific q values. This procedure can be expected to lead to reasonable results as far as the degeneracy of the eigenvalues shows up clearly enough to suggest a one-to-one relation to the corresponding values for q (in the present case up to $q \approx 0.2-0.3$), and becomes less and less reliable on increasing q .